Measurement of fibrous cap thickness in atherosclerotic plaques by spatiotemporal analysis of laser speckle images

Seemantini K. Nadkarni,
Massachusetts General Hospital, Harvard Medical School, Wellman Center for Photomedicine, Boston, Massachusetts 02114, snadkarni@hms.harvard.edu

Alberto Bilenca,
Massachusetts General Hospital, Harvard Medical School, Wellman Center for Photomedicine, Boston, Massachusetts 02114

Brett E. Bouma, and
Massachusetts General Hospital, Harvard Medical School, Wellman Center for Photomedicine, Boston, Massachusetts 02114

Guillermo J. Tearney
Massachusetts General Hospital, Harvard Medical School, Wellman Center for Photomedicine, Department of Pathology, Boston, Massachusetts 02114

Abstract

Necrotic-core fibroatheromas (NCFA) with thin, mechanically weak fibrous caps overlying lipid cores comprise the majority of plaques that rupture and cause acute myocardial infarction. Laser speckle imaging (LSI) has been recently demonstrated to enable atherosclerotic plaque characterization with high accuracy. We investigate spatio-temporal analysis of LSI data, in conjunction with diffusion theory and Monte Carlo modeling of light transport, to estimate fibrous cap thickness in NCFAs. Time-varying laser speckle images of 20 NCFAs are selected for analysis. Spatio-temporal intensity fluctuations are analyzed by exponential fitting of the windowed normalized cross-correlation of sequential laser speckle patterns to obtain the speckle decorrelation time constant, $\tau(\rho)$, as a function of distance ρ from the source entry location. The distance, ρ', at which $\tau(\rho)$ dropped to 65% of its maximum value is recorded. Diffusion theory and Monte Carlo models are utilized to estimate the maximum photon penetration depth, $z_{max}(\rho')$, for a distance equal to ρ', measured from LSI. Measurements of $z_{max}(\rho')$ correlate well with histological measurements of fibrous cap thickness ($R=0.78$, $p<0.0001$), and paired t-tests show no significant difference between the groups (p=0.4). These results demonstrate that spatio-temporal LSI may allow the estimation of fibrous cap thickness in NCFAs, which is an important predictor of plaque Stability.

Keywords

atherosclerosis; fibrous cap; diffusion; laser speckle

Address all correspondence to Seemantini K. Nadkarni, Massachusetts General Hospital, Harvard Medical School, Wellman Center for Photomedicine, Boston, Massachusetts 02114. Tel: 617–724–1381; Fax: 617–726–4103; snadkarni@hms.harvard.edu.

1 Introduction

The rupture of atherosclerotic plaque is a frequent precursor to thrombus-mediated acute coronary syndromes and is responsible for almost 75% of acute myocardial infarctions in patients.[1-5] One type of atherosclerotic plaque, the necrotic-core fibroatheroma (NCFA), is most commonly found at the site of coronary thrombosis in patients who have succumbed to sudden cardiac death.[6] Autopsy studies have demonstrated that NCFAs, which are comprised of a thin, mechanically weak fibrous cap overlying a compliant necrotic lipid-rich core, have a high propensity for rupture (Fig. 1).[6] The fibrous cap, predominantly composed of collagen and smooth muscle cells, is an important structural entity that determines the mechanical stability of the NCFA. It provides a protective envelope that shields the highly thrombogenic material in the necrotic core from contact with coagulation factors in the coronary blood circulation.[7] The onset of occlusive coronary thrombosis is initiated by the fracture of the fibrous cap, followed by the release of thrombogenic contents of the plaque into the circulation. Recent studies have shown that lipid-lowering therapy initiates dynamic remodeling of the plaque by causing a net increase in the collagen content and thickness of the fibrous cap, ultimately resulting in the stabilization of the plaque.[8-10] Due to its role in plaque stability, the fibrous cap is an important anatomic target for the detection of high-risk atherosclerotic plaques in patients.

Laser speckle imaging (LSI) is a new optical technique that has demonstrated high sensitivity and specificity for atherosclerotic plaque diagnosis.[11,12] In this technique, a focused coherent laser beam illuminates the plaque, time-varying laser speckle images are acquired, and the speckle pattern decorrelation times are computed. Since laser speckle patterns are modulated by the random Brownian motion of particles within the plaque, the measurement of speckle decorrelation times provides information on plaque viscoelasticity. In a previous study to demonstrate LSI for plaque characterization, speckle decorrelation time constants were found to be highly dependent on plaque type and composition, including lipid and collagen content.[11]

In this prior work, the decorrelation time constants were computed over the entire speckle pattern. As a result, the effects of Brownian motion were integrated over the illuminated volume, and depth-resolved spatial information was lost. Due to the diffusion properties of light propagation in tissue, photons returning from deeper regions within the tissue have a higher probability of remittance farther away from the illumination beam entry point.[13-16] By investigating speckle pattern decorrelation as a function of distance from the illumination beam entry point, it therefore should be possible to obtain information on plaque morphology as a function of depth. In this work, we consider this feature of LSI and explore its ability to estimate fibrous cap thickness in NCFAs. Using *ex vivo* studies, we investigate the possibility of combining spatio-temporal measurements of laser speckle fluctuations with diffusion theory of light propagation in tissues to obtain information about fibrous cap thickness.

2 Methods

2.1 Laser Speckle Imaging

Laser speckle imaging was conducted on thoracic and abdominal aortic segments, obtained from 14 human cadavers. Immediately after harvest, the aortas were stored in phosphate buffered saline (PBS) at 4°C. A total of 118 aortic plaques were randomly selected by gross examination, and imaging was performed within a PBS bath maintained at 37°C. The time between autopsy and imaging did not exceed 48 h.

A bench-top LSI system was constructed to acquire laser speckle images of aortic plaques *ex vivo*. Light from a polarized helium neon laser was reflected off a galvanometer mounted

mirror, expanded by 5:1, and then focused to a 75-μm-diam spot on the luminal surface of the plaque. The distance between the focusing lens and the aortic specimen was 13 cm. The computer-controlled galvanometer-mounted mirror enabled accurate positioning of the illumination beam over the center of the plaque. Cross-polarized laser speckle images were acquired using a charge-coupled device (CCD) camera (TM-6710CL, Pulnix, Sunnyvale, California). Time-varying laser speckle images were obtained from each imaging site at 240 frames/s for a duration of 2 s. To ensure accurate registration with histology, the right and left lateral edges of the remitted speckle pattern diameter were marked with India ink.

Following imaging, plaques were fixed in 10% formalin, embedded, and sectioned for histological processing. Sections were cut across the fiducial ink marks and stained with hematoxylin-eosin and Trichrome stains. The histological sections were interpreted by a pathologist blinded to the LSI data. Plaques that were histologically confirmed as NCFAs were selected for subsequent analysis. Morphometric measurements of fibrous cap thickness were obtained from the digitized histopathology slides. In each digitized histological image, the position of the illumination spot was delineated as the midpoint between the fiducial marks. Fibrous cap thickness was measured by starting at the midpoint and moving outward toward the fiducial marks on either side. The average fibrous cap thicknesses for the right and left portions of the NCFA were computed from cap thickness measurements performed at 200-μm spacings on either side of the illumination position. Hence for each NCFA, two histological measurements of average cap thickness were obtained, each corresponding to portions of the plaque to the right and left of the illumination site.

2.2 Laser Speckle Imaging - Monte Carlo Analysis

We have previously shown that the rate of speckle pattern decorrelation, governed by the Brownian motion of intrinsic particles, is dependent on the viscoelastic properties of the plaque, and hence the plaque composition. A NCFA, in simplest terms, can be described as a two-layered tissue with a stiffer fibrous layer, rich in collagen and smooth muscle cells, overlying a deeper core of lower viscosity comprising lipid and necrotic debris [Fig. 2(a)]. Based on Brownian motion considerations, we expect that the fibrous layer would affect a slower rate of speckle decorrctation (longer time constant) compared to the necrotic lipid layer (shorter time constant). Monte Carlo simulations and diffusion theory studies have shown that as photons travel deeper into tissue, they have a higher probability of being remitted farther away from the illumination location [14,17,18] [Fig. 2(a)]. Due to this effect, in a NCFA, when speckle decorrelation is measured as a function of radial distance, ρ, from the illumination location, a radially dependent time constant, $\tau(\rho)$, will be observed. In proximity to the illumination location, most photons will only have traversed the stiff, high-viscosity fibrous cap and the decorrelation times will be long. Farther away from the illumination site, the majority of photons will have propagated through the deeper low viscosity core, and the decorrelation times will therefore be shorter [Fig. 2(b)]. We hypothesize that the distance, ρ', at which this time constant transition occurs, will be correlated to the NCFA cap thickness (Fig. 2).

To lest this hypothesis, we analyzed the spatio-temporal characteristics of LSI data obtained from NCFAs. For each speckle image series, the position of the illumination spot, which was approximately at the center of the plaque, was manually located. Speckle decorrelation curves as a function of time were obtained for each value of ρ by performing a normalized 200×200-μm windowed cross-correlation centered at each ρ. Each window in the time series was correlated with the first image window (t=0) in the Fourier domain.[19] For each value of ρ, a normalized speckle decorrelation curve was created by extracting windowed cross-correlation maxima and normalizing them to the windowed autocorrelation maxima. The radially resolved decorrelation time constant $\tau(\rho)$ was computed by exponential fitting of the decorrelation curve for each ρ, and by moving the center of the window in $\Delta\rho$ increments of 50 μm. The window

was translated from the illumination spot to the ink mark locations for accurate registration with histology.

Due to tissue heterogeneity and variations in fibrous cap thickness, the measured laser speckle patterns were asymmetric; hence, we obtained two plots of $\tau(\rho)$ versus ρ corresponding to either side of the illumination location for each NCFA, and the inflection distance, ρ', is measured from each plot. Therefore, a total of 38 measurements from 19 NCFAs were obtained. We approximated that at distances smaller than ρ', the observed speckle pattern was predominantly affected by photon scattering within the fibrous cap (Fig. 2). Conversely, for distances greater than ρ', the observed speckle pattern was primarily affected by scattering in the necrotic core (Fig. 2). To determine the value of ρ that best approximates the inflection distance, ρ' was measured as the distance at which $\tau(\rho)$ dropped to the range of 80 to 40% of its maximum value τ_{max} at the illumination location. Therefore, multiple values of ρ' were determined over the range of thresholds of 80 to 40% of τ_{max}.

Next, we related the radial distance, ρ', measured for the range of thresholds of τ_{max} to the thickness of the fibrous cap, by combining a diffusion theory model of spatially resolved diffuse reflectance[20] and a Monte-Carlo model of light transport in tissue[14] to estimate the radially resolved maximum photon penetration depth through the NCFA fibrous cap. The tissue was described by its optical parameters: the absorption coefficient μ_a, the scattering coefficient μ_s, and the anisotropy coefficient g, as well as the refractive indices of air and tissue ($n = 1.4$). First, we derived the optical properties of fibrous tissue at 632 nm by measuring the radially dependent remittance from six atherosclerotic plaques, histologically confirmed as fibrous plaques. Fibrous plaques were utilized, as the optical properties of collagen in these plaques should closely resemble the optical properties of fibrous caps in NCFAs. Time-varying speckle images of the fibrous plaques were obtained using the imaging set up as described before. Given the quantum efficiency and gain of the CCD camera, the total number of diffuse photons remitted from the plaque and detected by the CCD sensor was measured by time-averaging speckle images acquired over a period of 2 s. The radially resolved photon probability $P(\rho)$ for each fibrous plaque was generated by summing the number of photons detected over different annuli of radii ρ, and then normalizing this value by the total number of photons detected over the area of the CCD detector. The theoretical radial photon probabilities calculated from a single-scatterer diffusion model for the case of a semi-infinite homogeneous tissue[20] were fitted to the measured radial photon probabilities, $P(\rho)$, by means of a least-square optimization procedure to extract the optical properties, μ_a, μ_s, and g, for each fibrous plaque. Next, we compared optical properties obtained from the librous plaques to that derived from time-averaged laser speckle images of five normal aortic tissue samples at 632-nm wavelength.

The optical properties of the fibrous plaques were used as inputs to a Monte Carlo model that assumed a semi-infinite homogeneous layer.[14] Photon initial conditions included input beams perpendicular to the semi-infinite layer. Multiple runs were performed with the same set of optical properties, and a total of 500,000 photon packet trajectories were launched. Remitted photons were collected over a radial distance of 2 mm. From the output of the Monte Carlo simulations, the radially resolved maximum penetration depth was recorded for each photon. The mean of the distribution of maximum penetration depths of photons remitted at a distance ρ provided an estimate of the mean maximum penetration depth, $z_{max}(\rho)$, as a function of radial distance.[14] Similarly, $z_{max}(\rho)$ look-up tables were obtained using Monte Carlo (MC) simulations for each of the six fibrous plaques. Finally, for each NCFA, ρ' was determined via spatio-temporal LSI as described before, and input into each of the six $z_{max}(\rho)$ look-up tables to obtain a parameter $z_{max}(\rho')$. The mean $\bar{z}_{max}(\rho')$ value was calculated for each NCFA as the average of six $z_{max}(\rho')$ values. Consequently, $\bar{z}_{max}(\rho')$ was calculated for ρ' corresponding to the range of inflection thresholds of τ_{max}. The parameter $\bar{z}_{max}(\rho')$ obtained using the combined LSI-MC technique for each NCFA was compared with the fibrous cap thickness measured by

histology using linear regression analyses and paired t-tests. For all analyses, a p-valuc <0.05 was considered statistically significant.

3 Results

3.1 Spatio-Temporal Laser Speckle Analysis

Twenty of the 118 atherosclerotic plaques that were imaged using LSI were histologically classified as NCFAs. One of the 20 NCFAs showed significant tearing of the fibrous cap in the histological section and was not used in the analyses. For the remaining 19 NCFAs analyzed in our study, the fibrous cap thicknesses measured by histology ranged from 85 to 715 μm. The average coefficient of variation given by the standard deviation in cap thickness measured between the fiducial marks expressed as a percentage of the mean was 26%. This implies that cap thickness measurements varied on average by 26% between the fiducials marks for the NCFAs analyzed in this study. Figure 3 shows examples in which the speckle decorrelation time constant $\tau(\rho)$ is plotted as a function of distance ρ from the illumination location for two NCFAs. In these plots, we see that $\tau(\rho)$ is approximately equal to 900 ms close to the illumination spot and drops with increasing distance ρ as the speckle pattern transitions to a more rapidly fluctuating pattern due to photon scattering in the necrotic core layer. In Fig. 3, the distance ρ' corresponding to 65% of τ_{max} is shown. The distances were $\rho' = 288$ μm for the NCFA with a histologically measured average cap thickness of 180± 13.1 μm, and $\rho' = 1080$ μm for an average cap thickness of 715±80 μm.

Figure 4 depicts one example of a 2-D colormap illustrating the spatial distribution of $\tau(\rho)$ measured by translating a 200×200-μm correlation window at 50-μm intervals across a 0.6×2-mm region of a necrotic core fibroatheroma. The doited line in the colormap demarcates the line along which the corresponding histological section was obtained. In the colormap, $\tau(\rho)$ is high at the center of the plaque corresponding to a thicker region of the fibrous cap, and rapidly drops as the cap thins out toward the peripheral regions of the NCFA.

3.2 Laser Speckle Imaging-Monte Carlo (LSI-MC) Analysis

Figure 5(a) shows one example of the radial photon probabilities, $P(\rho)$, measured experimentally for a fibrous plaque compared with the theoretical radial photon probabilities calculated from the diffusion model for a semi-infinite homogeneous tissue.[20] The average optical properties that we obtained by utilizing a least-squares optimization procedure to fit the theoretical curve to the experimental data yielded, for the fibrous plaques: $\overline{\mu_a}$=3.82 ± 0.31 cm^{-1}, $\overline{\mu_s}$=440.65 ± 0.11 cm^{-1}, and $\bar{g}$=0.8; and for the normal aortic samples: $\overline{\mu_a}$=3.92 ± 0.34 cm^{-1}, $\overline{\mu_s}$=403.18 ± 0.15 cm^{-1}, and $\bar{g} = 0.8$. These values correspond with previously published results of optical properties of the human aorta at 632-nm wavelength. [21] Figure 5(b) shows the results of the Monte Carlo simulations in which the average radially resolved photon penetration depth $\bar{z}_{max}(\rho)$, measured for six fibrous plaques, is plotted as a function of distance ρ from the illumination location. The error bars show the standard deviation. The plot shows that the uncertainty in estimating $\bar{z}_{max}(\rho)$ increases with distance from the illumination location.

Linear regression analysis demonstrated good correlation between $\bar{z}_{max}(\rho')$ and fibrous cap thickness measured from histology at ρ' evaluated over the entire range of inflection thresholds of τ_{max} (R=0.64 to R=0.78;p<0.0001). In Fig. 6, $\bar{z}_{max}(\rho')$, where ρ' is the radial distance at 65% of τ_{max}, is plotted versus the average fibrous cap thickness measured from histology. Within the threshold range, the parameter $\bar{z}_{max}(\rho')$ at ρ' corresponding to 65% of τ_{max} showed the strongest positive correlation with histological measurements (R=0.78, p<0.0001). In addition at the 65% inflection threshold, LSI-MC and hislological measurements of cap thickness showed the lowest difference in mean measurements between the groups. The results of the

paired t-tests showed that the least statistically significant difference between LSI-MC measurements of $\bar{z}_{\max}(\rho')$ and histological measurements of fibrous cap thickness for ρ' measured at 65% of $\tau_{\max}$ (p=0.4).

4 Discussion

In this work, we describe a new technique to obtain depth-resolved structural information about necrotic-core fibroatheromas by the spatio-temporal analysis of laser speckle patterns. This study demonstrates that by combining analyses of the second-order statistics of time-varying laser speckle fluctuations with diffusion theory and Monte Carlo models of light propagation in tissue, it may be possible to obtain an estimate of fibrous cap thickness in necrotic-core fibroatheromas, which is an important predictor of plaque vulnerability.

Due to the differences in viscoelastic properties of the fibrous cap layer and the necrotic core in a NCFA, the Brownian motion of particles within the two layers elicits differences in speckle intensity fluctuations resulting from photon scattering in each layer. By analyzing the spatial variation in the speckle pattern decollation time constant $\tau(\rho)$ as a function of distance ρ, from the source, we obtained the distance ρ' at which $\tau(\rho)$ dropped to 65% of its maximum value. Monte Carlo simulations enabled the determination of the maximum photon penetration depth $z_{\max}(\rho)$ as a function of radial distance from the source location. When $z_{\max}(\rho)$ was evaluated at ρ' (from LSI), we obtained the parameter $\bar{z}_{\max}(\rho')$ that was highly correlated to the average fibrous cap thickness measured from histological sections (R=0.78,p<0.0001). The results of the paired t-test demonstrated that the measurements of $\bar{z}_{\max}(\rho')$ were not significantly different from histological measurements, suggesting that LSI may provide a viable technique for the estimation of fibrous cap thickness in NCFAs. By analyzing the spatial dependence of $\tau(\rho)$, we have demonstrated that 2-D maps can be reconstructed to evaluate the variation in fibrous cap thickness across the NCFA (Fig. 4). Using these methods, it may be possible to illustrate regions of focal thinning within the fibrous cap to aid in identifying potential sites for plaque rupture. When combined with illumination beam scanning, this feature of LSI could enable the acquisition of 3-D volumetric maps of plaque morphology and viscoelasticity distributions.

In this work, the diffusion theory model of spatially resolved diffusive reflectance developed by Farell, Patterson, and Wilson was used for optical characterization of the aortic tissues.[20] By fitting the theoretical prediction of radially resolved photon probability to experimentally measured data, we extracted the optical properties for aortic fibrous plaques. In our study, the experimental measurements of photon probabilities were normalized with the theoretical curves by including a scaling factor. The scaling factor, determined using a least-squares fitting procedure, was included to account for imaging system parameters such as the limited solid angle of collection due to the finite aperture of the imaging lens system, the angle of the CCD camera (<20 deg) with respect to the tissue surface, and the sensitivity of the CCD camera. This study has shown that it is possible to characterize optical properties of tissue from analyses of laser speckle images with relative experimental ease. The technique thus lends itself to the possibility of optically characterizing different types of atherosclerotic plaques for a variety of research as well as clinical applications.

Although the LSI-MC technique shows good correlation with histological measurements of cap thickness, and there is no significant difference between these groups, the factors that may influence the precision of LSI-MC measurements are: 1. the distance ρ' beyond which speckle fluctuations are predominantly due to light scattering from the necrotic core; 2. the optical properties of the fibrous cap, which defines the accuracy of the MC calibration curve; and 3. the measurement of the average fibrous cap thickness in histological sections. The influence of these factors on LSI-MC measurements is described next.

As described before, ρ' was determined as the distance from the illumination location at which $\tau(\rho)$ dropped to a given percent of its maximum value τ_{max}. In our experiments, we evaluated the parameter $\bar{z}_{max}(\rho')$ for ρ' corresponding to different thresholds of τ_{max}. The endpoints of the threshold range were selected based on our empirical results. Within the threshold range of 80 to 40% τ_{max}, differences between LSI-MC measurements of $\bar{z}_{max}(\rho')$ were not statistically significant. At the endpoints of the range, i.e., at 80 and 40% of τ_{max}, LSI-MC measurements were significantly different from histological measurements (at 80% τ_{max}: p<0.01 and 40% τ_{max}: p<0.001). Based on these findings, we limited our range of thresholds between 80 to 40% τ_{max}. We found that LSI-MC measurements of $\bar{z}_{max}(\rho')$ evaluated for ρ' at 65% of τ_{max} showed the strongest correlation ($R=0.78, P<0.0001$) and the smallest statistically significant difference ($p=0.4$) with histological measurements. From these results, we may infer that ρ' evaluated at 65% of τ_{max} provided the best approximation of the inflection distance. However, the true inflection distance at which the speckle pattern transitions from the fibrous cap to the necrotic core may in fact be less than the measured inflection distance ρ'. The size of the cross-correlation window used to calculate the radially resolved value of $\tau(\rho)$ influences the determination of the true inflection distance, due to the blurring effect of the finite window on the $\tau(\rho)$ data. Hence, the measured $\tau(\rho)$ does not show a sharp drop at the inflection point, and instead, a smooth roll off of $\tau(\rho)$ is often observed as a function of ρ (Fig. 3). In our study, the 200×200-μm window size was selected empirically. The optimum size of the cross-correlation window may be influenced by the statistical uncertainty in detecting photons returning from depth, $z_{max}(\rho)$ remitted within the finite window centered at ρ. With future studies, it may be possible to optimize the size of the cross-correlation window by applying the results of MC simulations of radially resolved photon penetration depths to minimize the statistical uncertainty in detecting photons remitted within a finite window. Thus, by optimizing the size of the cross-correlation window, it may be possible to obtain increased spatial resolution in measuring $\tau(\rho)$, and the inflection distance may be determined more precisely.

The diffusion theory and Monte Carlo models in this study characterize only the fibrous cap of the NCFA, by describing a single-layered, semi-infinite, homogeneous medium. A more accurate representation of the NCFA would involve a two-layered model with different sets of optical properties to describe the fibrous cap and the necrotic core. However, the measurement of optical properties of the necrotic core can be a challenging task, as the core can be extremely heterogeneous in composition, consisting of lipid, collagen fibrils, cholesterol crystals, inflammatory cells, and necrotic debris. Furthermore, the optical properties of the necrotic core may vary considerably across plaques and across patients, and as a result may be difficult to characterize. In our analyses, we utilize a spatio-temporal LSI technique to determine the distance ρ'. We can approximate that photons remitted at distances greater than ρ' have exited through the fibrous cap and propagated into the necrotic core. Likewise, photons remitted at distances less than ρ' have predominantly traversed only through the fibrous cap. Since the fibrous cap can be assumed as a single-layered homogeneous medium, and by measuring the maximum photon penetration depth $z_{max}(\rho')$, only through this fibrous medium constrained by a distance ρ' from the source, we utilized a simplified model of the fibrous cap and did not require characterizing the optical properties of the necrotic core.

For ease of implementation, we only measured optical properties using six collagen-rich fibrous plaques in the present study. Although we have not investigated the intra-plaque and intra-patient differences in the optical properties of the aortic fibrous tissue, we expect that these differences may be negligible, as the fibrous cap predominantly consists of collagen. However, for successful *in vivo* application, it may be important to develop a fibrous cap model by analyzing several fibrous plaques, to investigate the variation of optical parameters due to fibrous cap constituents such as collagen types 1 and 3, the presence of smooth muscle cells, and macrophages. Further investigation of such a model would reduce the statistical uncertainty in determining the optical properties of the fibrous cap, thereby enabling future spatio-temporal

LSI measurements of fibrous cap thickness with increased precision. In addition, we observed that the optical properties of fibrous plaques did not differ significantly from those measured from normal aortic tissue samples, in spite of possible differences in the compositions of the two tissue types. In a fibrous plaque, laser speckle images would mainly be influenced by light scattering within an extensively thickened intimal layer (>500 μm) predominantly consisting of collagen. However, the adult aorta, which may appear normal on gross examination, often shows intimal hyperplasia (thickening of the intima up to 500 μm) with increased deposition of collagen and smooth muscle cell proliferation in the intima. Due to intimal hyperplasia, laser speckle fluctuations may similarly be influenced by scattering within the thick intimal as well as the medial layers. As a result, optical properties measured from time-averaged speckle images of the fibrous plaque and normal aorta may not be significantly different in our study.

Registration of speckle images with the corresponding histology was performed using ink marks on the lesion site. Since fibrous cap thickness may vary as a function of measurement location, registration errors between speckle and histology images could affect LSI results. Since cadaveric specimens were used in the study and were stored in PBS for up to 48 h before imaging, minor degradation of the specimen may have occurred. The effect of tissue degradation on the optical properties of plaques was not tested in this study. However, previous experience with other optical imaging techniques in our laboratory suggest that the optical properties of vascular tissue undergo only minor changes as long as the measurements are performed within 48 h of autopsy.

In our study, although speckle images were acquired over a 2-s duration, $\tau(\rho)$ measurements were performed by single exponential fitting of the region of the normalized speckle decorrelation curve, over which the cross-correlation value dropped to 75% of its maximum, corresponding to an average acquisition time of less than 100 ms. For future *in viva* applications, this relatively short acquisition time requirement would allow for a sufficient temporal window during the resting phase of the cardiac cycle to obtain diagnostic quality speckle data. In addition, a CCD camera with a significantly higher image acquisition rate could be used to provide higher temporal resolution of time-varying speckle data, which may allow for measurements of speckle decorrelation to be performed over a few milliseconds. We have already demonstrated in our previous study that LSI measurements can be obtained with high accuracy even under physiological rates of maximal arterial deformation.[11]

LSI may be extended to patient studies by using small diameter flexible optical fiber bundles, similar to those of coronary angioscopy, to obtain laser speckle images of coronary plaques. [22,23] Intracoronary saline flushing, which has been successfully implemented in *in vivo* optical coherence tomography and angioscopy procedures to temporarily displace blood by injecting a bolus of saline, can be utilized in conjunction with LSI to enable unobstructed imaging of the coronary wall.[24,25]

LSI is a unique technique, as it enables plaque characterization by providing measurements that are related to the viscoelastic properties of atherosclerotic lesions. It has been previously demonstrated that at a single beam location, LSI can identify plaque type and measure an index of viscoelasticity that is related to plaque composition. In this study, we have demonstrated the ability of LSI to provide depth-resolved information. By combining LSI measurements of the spatial variation in decorrelation time constants with a Monte Carlo model to describe light propagation through the plaque, it is possible to measure a parameter that is highly correlated with fibrous cap thickness, which is a critical anatomical predictor of plaque rupture. Based on its unique ability to provide both biomechanical and structural information, we anticipate that catheter-based LSI will become a powerful tool for detecting high risk lesions to target local therapy prior to the onset of an acute coronary event.

Acknowledgments

References

1. Lee RT, Libby P. The unstable atheroma. Arterioscler, Thromb, Vasc Biol 1997;17:1859–1867. [PubMed: 9351346]

2. Libby P. Molecular bases of the acute coronary syndromes. Circulation 1995;91:2844–2850. [PubMed: 7758192]

3. Falk E, Shah PK, Fuster V. Coronary plaque disruption. Circulation 1995;92:657–671. [PubMed: 7634481]

4. Muller JE, Tofler GH, Stone PH. Circadian variation and triggers of onset of acute cardiovascular disease. Circulation 1989;79:733–743. [PubMed: 2647318]

5. Arroyo LH, Lee RT. Mechanisms of plaque rupture: mechanical and biologic interactions. Cardiovasc Res 1999;41:369–375. [PubMed: 10341836]

6. Virmani R, Kolodgie FD, Burke AP, Farb A, Schwartz SM. Lessons from sudden coronary death: a comprehensive morphological classification scheme for atherosclerotic lesions. Arterioscler, Thromb, Vasc Biol 2000;20:1262–1275. [PubMed: 10807742]

7. Fernandez-Ortiz A, Badimon JJ, Falk E, Fuster V, Meyer B, Mailhac A, Weng D, Shah PK, Badimon L. Characterization of the relative thrombogenicity of atherosclerotic plaque components: implications for consequences of plaque rupture. J Am Coll Cardiol 1994;23:1562–1569. [PubMed: 8195515]

8. Libby P, Aikawa M. Mechanisms of plaque stabilization with statins. Am J Cardiol 2003;91:4B–8B.

9. Aikawa M, Rabkin E, Okada Y, Voglic SJ, Clinton SK, Brinckerhoff CE, Sukhova GK, Libby P. Lipid lowering by diet-reduces matrix metalloproteinase activity and increases collagen content of rabbit atheroma: a potential mechanism of lesion stabilization. Circulation 1998;97:2433–2444. [PubMed: 9641696]

10. Libby P, Aikawa M. Stabilization of atherosclerotic plaques: new mechanisms and clinical targets. Nat Med 2002;8:1257–1262. [PubMed: 12411953]

11. Nadkarni SK, Bouma BE, Helg T, Chan RC, Halpern E, Chau A, Minsky M, Motz J, Houser SL, Tearney GJ. Characterization of atherosclerotic plaques by laser speckle analysis. Circulation. in press.

12. Tearney GJ, Bouma BE. Atherosclerotic plaque characterization by spatial and temporal speckle pattern analysis. Opt Lett 2002;27:533–535. [PubMed: 18007856]

13. Gonik MM, Mishin AB, Zimnyakov DA. Visualization of blood microcirculation parameters in human tissues by time-integrated dynamic speckles analysis. Ann NY Acad Sci 2002;972:325–330. [PubMed: 12496036]

14. Wang L, Jacques SL, Zheng L. MCML–Monte Carlo modeling of light transport in multi-layered tissues. Comput Methods Programs Biomed 1995;47:131–146. [PubMed: 7587160]

15. Sadhwanj A, Schomacker KT, Tearney GJ, Nishioka NS. Determination of teflon thickness with laser speckle. 1. Potential for burn depth diagnosis. Appl Opt 1996;35:5727–5735.

16. Boas DA, Nishimura G, Yodh AG. Diffusing temporal light correlation for burn diagnosis. Proc SPIE 1999;2979:468–474.

17. Flock ST, Patterson MS, Wilson BC, Wyman DR. Monte Carlo modeling of light propagation in highly scattering tissue–I: Model predictions and comparison with diffusion theory. IEEE Trans Biomed Eng 1989;36:1162–1168. [PubMed: 2606490]

18. Flock ST, Wilson BC, Patterson MS. Monte Carlo modeling of light propagation in highly scattering tissues–II: Comparison with measurements in phantoms. IEEE Trans Biomed Eng 1989;36:1169–1173. [PubMed: 2606491]

19. Lewis JP. Fast template matching. Vision Interface 1995:120–123.

20. Farell TJ, Patterson MS, Wilson BC. A diffusion theory model of spatially resolved, steady-state diffuse reflectance for the noninvasive determination of tissue optical properties *in vivo*. Med Phys 1992;19:879–888. [PubMed: 1518476]

21. Keijzer M, Richards-Kortum R, Jacques SL, Feld MS. Fluorescence spectroscopy of turbid media: autofluorescence of the human aorta. Appl Opt 1989;28:4286–4292. [PubMed: 20555864]

22. Kawasaki M, Takatsu H, Noda T, Sano K, Ito Y, Hayakawa K, Tsuchiya K, Arai M, Nishigaki K, Takemura G, Minatoguchi S, Fujiwara T, Fujiwara H. *In vivo* quantitative tissue characterization of human coronary arterial plaques by use of integrated back-scatter intravascular ultrasound and comparison with angioscopic findings. Circulation 2002;105:2487–2492. [PubMed: 12034654]

23. Uchida Y, Fujimori Y, Hirose J, Oshima T. Percutaneous coronary angioscopy. Jpn Heart J 1992;33:271–294. [PubMed: 1522685]

24. Jang IK, Bouma BE, Kang D II, Park SJ, Park SW, Seung KB, Choi KB, Shishkov M, Schleudorf K, Pomerantsev E, Houser SL, Aretz HT, Tearney GJ. Visualization of coronary atherosclerotic plaques in patients using optical coherence tomography: comparison with intravascular ultrasound. J Am Coll Cardiol 2002;39:604–609. [PubMed: 11849858]

25. MacNeill BD, Jang IK, Bouma BE, Iftimia N, Takano M, Yabushita H, Shishkov M, Kauffman CR, Houser SL, Aretz HT, DeJoseph D, Halpern EF, Tearney GJ. Focal and multi-focal plaque macrophage distributions in patients with acute and stable presentations of coronary artery disease. J Am Coll Cardiol 2004;44:972–979. [PubMed: 15337206]

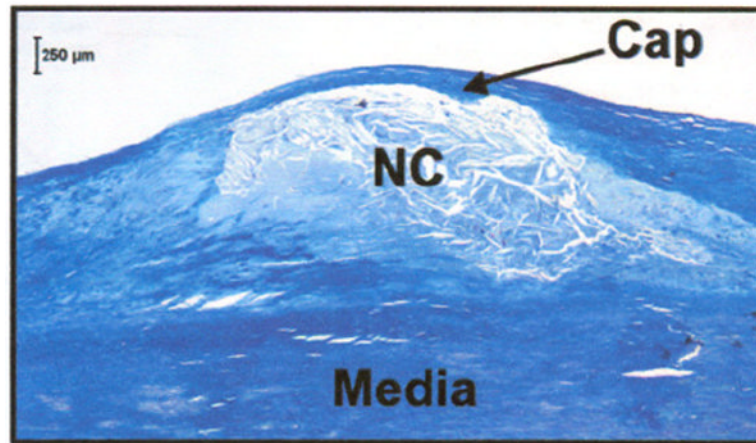**Fig. 1.**
Histological section showing a necrotic core fibroatheroma (NCFA) with a thin fibrous cap (arrow) overlying a large necrotic lipid core (NC). The fibrous cap, predominantly composed of collagen and smooth muscle cells, is an important structural entity that determines the mechanical stability of the NCFA. Masson's trichrome; original magnification 40×. Scale bar, 250 μm.

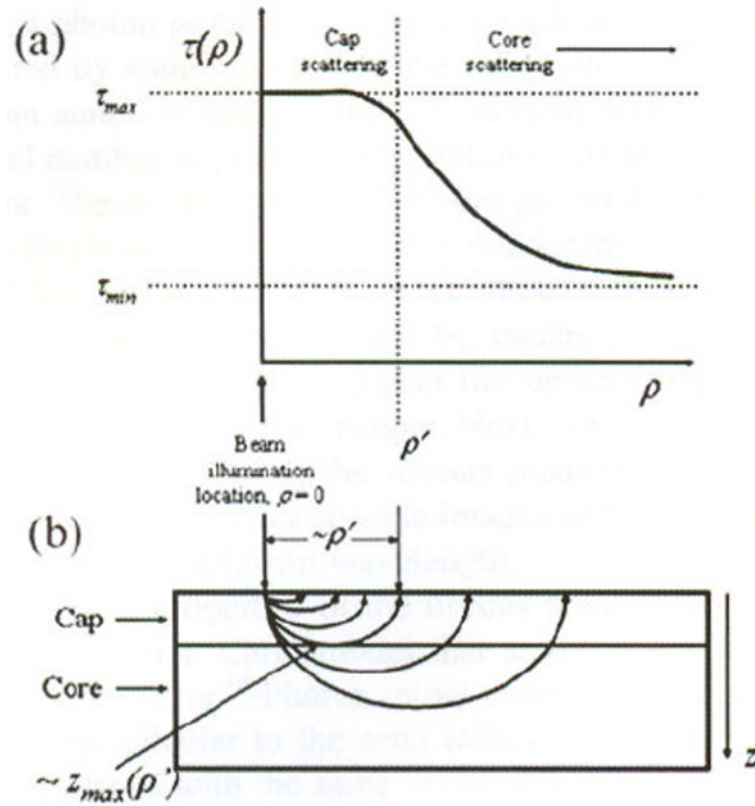**Fig. 2.**
(a) Radially resolved speckle decorrelation time constant $\tau(\rho)$ is polled versus distance ρ from the source. The inflection distance ρ' is shown in the polt. At distances less than ρ', most photons will only have traversed the fibrous cap and the decorrelation times will be higher. In contrast, at distances greater than ρ', the majority of photons will have propagated through the necrotic core and the decorrelation time will be shorter. (b) Schematic of photon propagtion through two-layer model demonstrating the approximate location of ρ' and $z_{max}(\rho')$.
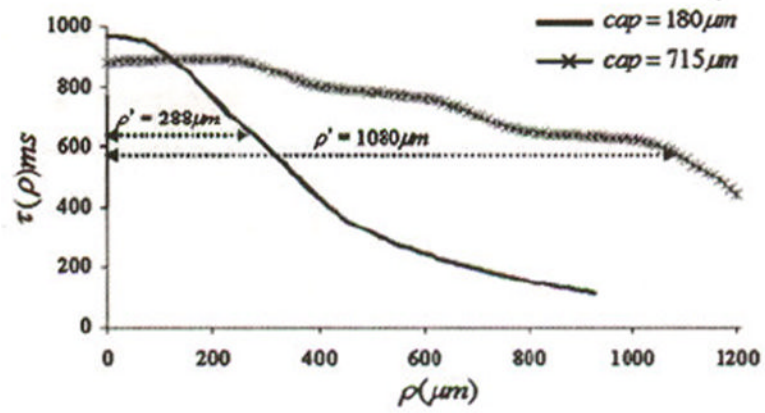
Fig. 3.
The figure shows $\tau(\rho)$ plotted versus distance ρ from the source entry point for two NCFAs with different cap thicknesses. The distance ρ' at which $\tau(\rho)$ drops to 65% of its maximum value is shown, which is related to the cap thickness.
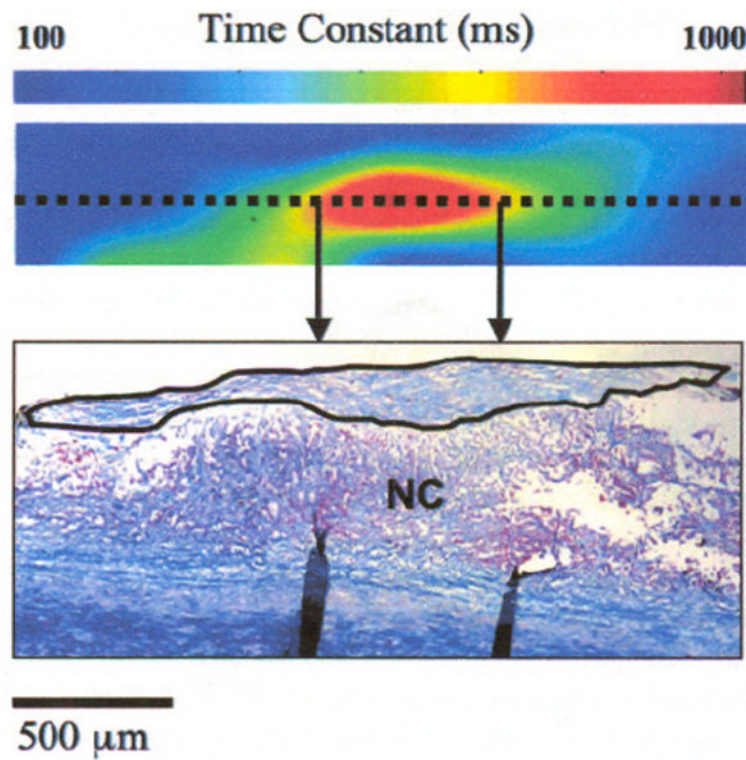
Fig. 4.
The colormap shows the spatial distribution of speckle decorelation time constants measured across a 0.6×2-mm region of a NCFA. The corresponding histological scetion obtained across the dotted line is shown in the figure, with the fibrous cap demarcated by the solid black line. A high decorrelation time constant (~900 ms) is measured at the center of the colormap corresponding to a thicker portion of the fibrous cap at the center of the NCFA, which rapidly drops (<100 ms) at the periphery of the colormap where the fibrous cap is very thin.
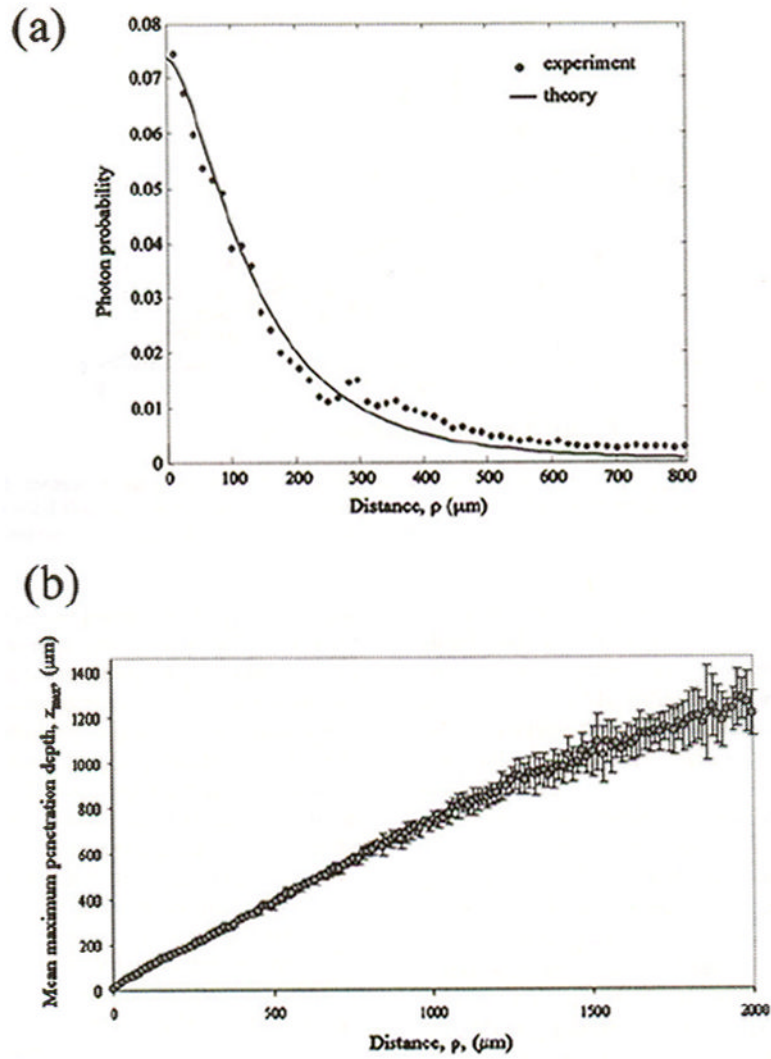
Fig. 5.
(a) Photon probability, measured from time-averaged speckle images of a fibrous plaque, is plotted as a function of distance ρ from the illumination location. Optical properties of the fibrous plaque were extracted by using a least-squares optimization procedure to fit the theoretical model to experimental data. The measured optical properties were: μ_a=5.36 cm^{-1}; μ_s=470.14 cm^{-1}; and g=0.8 for this fibrous plaque. (b) The maximum photon penetration depth $\bar{z}_{\max}(\rho)$ obtained from the Monte Carlo simulations using optical properties of six fibrous plaques, is plotted as a function of ρ.
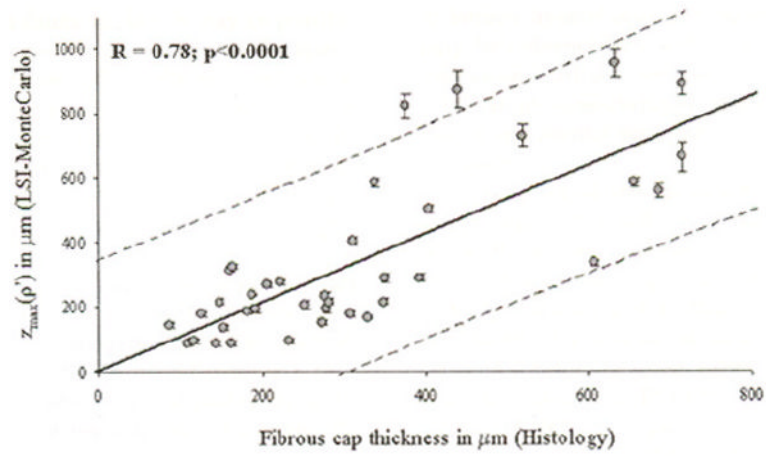
Fig. 6.
The parameter $\bar{z}_{\max}(\rho')$, measured using the LSI-MC technique for ρ' corresponding to 65% $\tau_{\max}$, is plotted against fibrous cap thickness mesured from histoloty. The soild line depicts the linear least-squares fit through the data, and the dotted lines show the 95% prediction limits. A high correlation was observed between $\bar{z}_{\max}(\rho')$ and NCFA fibrous cap thicknesses.